# Differential Content of Vesicular Glutamate Transporters in Subsets of Vagal Afferents Projecting to the Nucleus Tractus Solitarii in the Rat

Sam M. Hermes, James F. Colbert, and Sue A. Aicher*

Department of Physiology and Pharmacology, Oregon Health and Science University, Portland, Oregon 97239-3098

## ABSTRACT

The vagus nerve contains primary visceral afferents that convey sensory information from cardiovascular, pulmonary, and gastrointestinal tissues to the nucleus tractus solitarii (NTS). The heterogeneity of vagal afferents and their central terminals within the NTS is a common obstacle for evaluating functional groups of afferents. To determine whether different anterograde tracers can be used to identify distinct subpopulations of vagal afferents within NTS, we injected cholera toxin B subunit (CTb) and isolectin B4 (IB4) into the vagus nerve. Confocal analyses of medial NTS following injections of both CTb and IB4 into the same vagus nerve resulted in labeling of two exclusive populations of fibers. The ultrastructural patterns were also distinct. CTb was found in both myelinated and unmyelinated vagal axons and terminals in medial NTS, whereas IB4 was found only in unmyelinated afferents. Both tracers were observed in terminals with asymmetric synapses, suggesting excitatory transmission. Because glutamate is thought to be the neurotransmitter at this first primary afferent synapse in NTS, we determined whether vesicular glutamate transporters (VGLUTs) were differentially distributed among the two distinct populations of vagal afferents. Anterograde tracing from the vagus with CTb or IB4 was combined with immunohistochemistry for VGLUT1 or VGLUT2 in medial NTS and evaluated with confocal microscopy. CTb-labeled afferents contained primarily VGLUT2 (83%), whereas IB4-labeled afferents had low levels of vesicular transporters, VGLUT1 (5%) or VGLUT2 (21%). These findings suggest the possibility that glutamate release from unmyelinated vagal afferents may be regulated by a distinct, non-VGLUT, mechanism. J. Comp. Neurol. 522:642–653, 2014.



**INDEXING TERMS:** vesicular glutamate transporter; isolectin B4; cholera toxin B subunit; vagus nerve; electron microscopy; confocal microscopy

The vagus nerve contains primary visceral afferents that convey sensory information from cardiovascular, pulmonary, and gastrointestinal tissues to the nucleus tractus solitarii (NTS; Kalia and Mesulam, 1980; Kalia and Sullivan, 1982; Andresen and Kunze, 1994). These afferents are a mixed population of myelinated and unmyelinated fibers that carry a wide variety of information centrally (Mei et al., 1980). Recent studies indicate that the function and signaling of myelinated and unmyelinated vagal afferents may be quite distinct (Peters et al., 2010). Therefore, we first sought to determine whether vagal afferents could be parsed into myelinated and unmyelinated afferents with neuroanatomical tract tracing techniques. Cholera toxin B (CTb) has been used to label select afferent populations (Okada et al., 1982). The ganglioside GM1 on neuronal membranes has been shown to be the site of CTb binding and is responsible for facilitating transmembrane movement of CTb (Fishman, 1982). Based on somatic size within peripheral ganglia, as well as ultrastructural analysis, CTb has been shown to be an effective transganglionic tracer that reliably labels primarily medium-sized to large myelinated afferents, but has been reported to occasionally also label a small subset of unmyelinated afferents (Sugimoto et al., 1997; Corbett



Grant sponsor: National Institutes of Health; Grant number: R01 HL056301; Grant number: S10 RR016858 (confocal microscope); Grant number: P30 061800; Grant sponsor: Murdock Charitable Trust (electron microscope).

*CORRESPONDENCE TO: Sue Aicher, PhD, Oregon Health and Science University, Department of Physiology and Pharmacology, 3181 Sam Jackson Park Road, Mailcode: L334, Portland, OR 97239-3098. E-mail: aichers@ohsu.edu

Received March 28, 2013; Revised May 15, 2013;
Accepted July 11, 2013.
DOI 10.1002/cne.23438
Published online July 29, 2013 in Wiley Online Library (wileyonlinelibrary.com)

et al., 2005). In contrast, isolectin B4 (IB4), another transganglionic anterograde tracer, has been shown to bind specifically to alpha-D-galactose groups, allowing for identification of a subpopulation of unmyelinated primary afferents (Kitchener et al., 1993; Wang et al., 1994; Corbett et al., 2005). IB4 is believed to label primarily nonpeptidergic unmyelinated c-fibers in somatic nerves (Ambalavanar and Morris, 1993; Caterina and Julius, 1999). In contrast to somatic afferents, the distribution of these two tracers with respect to visceral vagal afferents and the capacity to utilize them to label distinct populations of vagal afferents is unknown. By using confocal and ultrastructural analyses, we determined that these two tracers label largely different populations.

Vagal afferents form primarily asymmetric synapses with neuronal targets in the NTS (Aicher et al., 1999), suggestive of excitatory neurotransmission, and glutamate is thought to be the primary excitatory neurotransmitter at the first primary afferent synapse in NTS (Talman et al., 1980). Vesicular glutamate transporters (VGLUTs) are believed to be located on synaptic vesicles and to play a role in the transport of glutamate into these vesicles (Renick et al., 1999; Bellocchio et al., 2000; Varoqui et al., 2002; Fremeau et al., 2004). It has been suggested that VGLUTs may be required for functional vesicular glutamate release from central axon terminals (Varoqui et al., 2002). Three glutamate transporters have been identified, VGLUT1, VGLUT2, and VGLUT3, and are generally expressed in nonoverlapping populations in the CNS (Fremeau et al., 2004). VGLUT1 and VGLUT2 share sequence similarity and are generally found in a complementary distribution throughout the brain and spinal cord (Fremeau et al., 2004). VGLUT3 does not share sequence similarity with the other two transporters, exhibits a much more variable localization, has been found in cholinergic as well as glutamatergic neurons (Gras et al., 2002; Fremeau et al., 2004; Takamori, 2006), and has not been reported in primary afferent fibers. Therefore, we confined our analysis to VGLUT1 and VGLUT2, which have been found in distinct populations of somatic afferents to dorsal horn (Todd et al., 2003; Alvarez et al., 2004). By combining immunohistochemistry for the two vesicular glutamate transporters with CTb and IB4 tract tracing, we attempted to determine whether there was a differential distribution of glutamate transporters to myelinated or unmyelinated vagal afferents projecting to NTS.

## MATERIALS AND METHODS

### Animals and surgery

Male Sprague-Dawley rats (n = 9, 250–430 g; Taconic Farms, Germantown, NY) were utilized for these experiments, and all protocols were in accordance with the Institutional Animal Care and Use Committee at Oregon Health and Science University. Vagal afferents were identified by using anterograde tracing following injection of CTb (1–2 μl; 1% in $dH_2O$; List Biological Laboratories, Campbell, CA) or lectin from *Bandeiraea simplicifolia* (IB4, 1–2 μl; 4% in $dH_2O$; Sigma-Aldrich, St. Louis, MO) into the left vagus nerve. Each rat was given atropine (0.1 mg/ml s.c.; Sigma-Aldrich) 15 minutes prior to surgery (to reduce bronchial and salivary secretions during surgery) and laid supine, and the left vagus nerve was isolated from surrounding tissues. A small piece of parafilm was placed under the cervical vagus to prevent leakage of the injectate into surrounding tissues. A glass micropipette (20–40 μm tip size) was inserted under the sheath of the left cervical vagus, and tracer was pressure injected using a picospritzer (General Valve Inc., Fairfield, NJ). Six rats received injections of either IB4 or CTb, and three rats received injections of both IB4 and CTb into the same nerve. After the injection, the parafilm was removed, and surgical wounds were sutured. The rat was monitored during recovery from anesthesia, then returned to the colony.

### Perfusion and immunocytochemistry

Seven days after injections, rats were overdosed with sodium pentobarbital (150 mg/kg) and perfused transcardially with the following solutions: 1) 10 ml heparinized saline, 2) 50 ml 3.8% acrolein in 2% paraformaldehyde, and 3) 200 ml 2% paraformaldehyde (in 0.1 M phosphate buffer [PB; pH 7.4]). The medulla was sectioned (40 μm) on a vibrating microtome (Leica, Malvern, PA) and collected into 0.1 M PB. Alternate sections from IB4- or CTb-injected cases were processed using immunoperoxidase detection for EM analysis. Sections were immersed in cryoprotectant solution (25% sucrose, 3% glycerol in 0.05 M PB) for 30 minutes and then briefly immersed in Freon, followed by liquid nitrogen. This "freeze-thaw" method increases penetration of antibodies into the surface of the tissue with a minimal disruption of morphology (Aicher et al., 1997, 1999). Tissue sections were then incubated for 30 minutes in a polyclonal goat primary antibody directed against either IB4 (1:1,000; Vector Laboratories, Burlingame, CA) or CTb (1:25,000; List Biological Laboratories) for 40 hours at 4°C. Sections were rinsed and incubated with a biotinylated horse anti-goat IgG (1:400; Vector Laboratories) for 30 minutes at room temperature and visualized with diaminobenzidine (DAB) precipitate. All incubations, except the primary antibody incubation, were carried out at room temperature with continuous agitation, and sections were rinsed between

TABLE 1.
Antibodies Used

| Host | Antibody | Source | Immunogen |
|---|---|---|---|
| Goat | Anti-isolectin B4 (1:1,000) | Vector Laboratories, Burlingame, CA (AS-2104) | *Griffonia (Bandeiraea) simplicifolia* lectin (GSL) I |
| Goat | Anti-CTb (1:25,000) | List Biological Laboratories, Campbell, CA (703) | Purified cholera toxin beta subunit |
| Rabbit | Anti-CTb (1:10,000) | Novus Biologicals, Littleton, CO (ab13612) | Purified choleragenoid |
| Guinea pig | Anti-VGLUT1 (1:5,000) | Millipore, Billerica, MA (ab5905) | Synthetic peptide corresponding to amino acid residues 542–560 of rat VGLUT1 (GATHSTVQPPRPPPPVRDY) |
| Guinea pig | Anti-VGLUT2 (1:2,500) | Millipore (ab5907) | Synthetic peptide corresponding to amino acid residues 565–582 of rat VGLUT2 (VQESAQDAYSYKDRDDYS) |

incubations in 0.1 M Tris-saline, pH 7.6 (3 × 5 minutes). The primary antibody incubation buffer also contained 0.1% bovine serum albumin (BSA).

After the immunoperoxidase procedure, tissue sections were fixed for 1 hour in 2.0% osmium tetroxide in 0.1 M PB, washed for 10 minutes in 0.1 M PB, dehydrated through a graded series of ethanols, then propylene oxide, and then propylene oxide:EMBed (1:1) solution overnight. Sections were then incubated in EMBed for 2 hours, embedded between two sheets of Aclar plastic, and placed in an oven for 48 hours at 60°C.

Remaining NTS sections were processed for combined immunofluoresence of both tracers in dually injected animals or the appropriate tracer and either VGLUT1 or VGLUT2. Sections were incubated first in 1% sodium borohydride solution for 30 minutes to increase antigenicity and then in 0.5% BSA for 30 minutes to reduce nonspecific binding. Tissue sections were incubated in polyclonal guinea pig primary antibodies directed against transporter-specific peptides for either VGLUT1 (1:5,000; Chemicon, Temecula, CA) or VGLUT2 (1:2,500; Chemicon) for 40 hours at 4°C. Bound antibodies were visualized with donkey secondary antibodies conjugated to Alexa 488, Alexa 546 (1:800; Molecular Probes, Eugene, OR), or Cy5 (1:800; Jackson Immunoresearch, West Grove, PA). For dual anterograde labeling cases, CTb was detected using a rabbit primary antibody (1:10,000; Novus Biologicals, Littleton, CO). Both the rabbit and the goat primary CTb antibodies exhibited very similar patterns of labeling. All incubations, except for the primary antibody incubation, were carried out at room temperature with continuous agitation, and sections were rinsed between incubations in 0.1 M Tris-saline (3 × 5 minutes). The primary antibody incubation buffer also contained 0.1% BSA. Sections were mounted onto gelatin-coated slides, coverslipped with Prolong Antifade Media (Molecular Probes), and stored at −20°C.

## Antibody characterization

Commercially available antibodies were used for this study (Table 1). The goat anti-CTb antibody was generated with purified cholera toxin beta subunit as the immunogen (per manufacturer specification) and has been previously utilized in other studies (Lefler et al., 2008; Hegarty et al., 2010). Preadsorption with 1 μg/ml and 5 μg/ml of CTb abolished all immunostaining of this antibody (Llewellyn-Smith et al., 1995). Per the manufacturer's specifications, the rabbit anti-CTb antibody was generated using purified choleragenoid as the immunogen. After injections of CTb into the cervical vagus, CTb immunoreactivity of both the goat and rabbit anti-CTb antibodies was identified in the brainstem within the NTS as well as the dorsal motor nucleus of the vagus (DMV). The antigen was not detected in cases without injections or in brain regions contralateral to the injection site. The distinct, specific immunoreactive pattern demonstrated by both CTb antibodies suggests it is unlikely that these antibodies bound nonspecifically to endogenous epitopes in the brainstem.

Per the manufacturer's specification, the IB4 antibody was raised in goat against the immunogen *Griffonia (Bandeiraea) simplicifolia* lectin (GSL) I. This antibody has been widely characterized in prior publications (Shehab, 2009; Starkey et al., 2009). The antigen was not detected in tissues lacking tracer injections or in brain regions contralateral to the injection site. Tissue sections incubated in primary antibodies directed against either CTb or IB4 without prior tracer application did not exhibit immunoreactivity.

Both VGLUT antibodies were raised in guinea pig against immunogens specific to each transporter. The immunogen for anti-VGLUT1 was a peptide corresponding to amino acid residues 542–560 of rat VGLUT1 (Melone et al., 2005; Ramer, 2008a), and the immunogen for anti-VGLUT2 was a peptide corresponding to

amino acid residues 565–582 of rat VGLUT2 (Schnell and Wessendorf, 2008; Ramer, 2008b). The specificity of these antibodies has been previously validated, and these antibodies have also been widely utilized (Chomsung et al., 2008; Hegarty et al., 2010). Immunoreactivity was absent from control experiments with either no primary antibody or mismatched primary and secondary antibodies. The specificity of the secondary antibodies was confirmed by incubating sections of brainstem with a particular primary antibody (for example, guinea pig anti-VGluT1), followed by a mismatched secondary antibody (for example, Alexa Fluor 488-conjugated donkey anti-goat). There was no immunoreactivity in any of the mismatch combinations tested.

### Electron microscopy

Regions of NTS at the level of the area postrema that contained labeling were glued to plastic blocks formed in Beem capsules (Pickel, 1981), and ultrathin sections (75 nm) were selected from an area just below the surface of the tissue at the tissue/plastic interface, where the penetration of antibodies is optimal (Aicher et al., 1995, 1999), and collected onto copper grids. The thin sections were counterstained with uranyl acetate and Reynolds lead citrate, and images were captured on a Tecnai 12 TEM (FEI, Hillsboro, OR) using a digital camera (Advanced Microscopy Techniques, Danvers, MA; 2.6K $\times$ 2.6K). Labeled structures and their contacts were classified based on morphological features (Peters et al., 1991; Aicher et al., 1999). Myelinated axons were identified by multiple layers of myelin sheath, whereas unmyelinated axons typically were found in bundles and lacked a myelin sheath. Axon terminals contained small clear vesicles as well as mitochondria and often formed appositions with dendrites. Synapses were classified as asymmetric if vesicles were clustered near the presynaptic membrane and a prominent density was present on the postsynaptic side of the contact. Electron micrographs used for publication were adjusted for optimal brightness and contrast in Adobe Photoshop (CS5), and figures were created in Adobe Illustrator (CS5).

### Confocal imaging

Z stacks bounded by the vertical extent of the labeling within NTS were captured using the single-pass, multitracking format on an LSM 510 confocal microscope (Zeiss, Thornwood, NY). A 488-nm laser (argon/2), a 543-nm (HeNe1) laser, and a 633-nm laser (HeNe2) were used to excite Alexa Fluor 488, Alexa Fluor 546, and Cy5, respectively. Emitted wavelengths passed through an HFT UV/488/543/633-nm dichroic mirror and then the appropriate bandpass filter sets, 500–550 nm for Alexa Fluor 488, 565–615 nm for Alexa Fluor 546, and 650–710 nm for Cy5, before collection. Control images were captured with excitation parameters for the fluorophores on the tissue sample not of interest, with the collection parameters for the Alexa Fluor of interest to assess bleed through the channels. All controls were blank. Consecutive optical sections (optical thickness 0.9 μm) were separated by an interval of 0.5 μm. Confocal micrographs used for publication were adjusted for optimal brightness and contrast in Zeiss ZEN software, and figures were created in Adobe Illustrator (CS5).

### Quantification and analysis

To determine whether CTb and IB4 were colocalized, 20 IB4-labeled varicosities and segments of fibers within each vibratome section of medial NTS per rat (n = 3, total of 60 IB4-labeled varicosities) were examined. In the same area, of the same sections, 50 CTb-labeled varicosities per rat (n = 3, total of 150 CTb-labeled varicosities) were examined. Varicosities were operationally defined as a discrete region, twice the diameter of the fiber of origin (Bailey et al., 2006). For these studies, we defined colocalization as overlapping morphology of the varicosity with labeling for the other tracer in at least two adjacent optical sections. Each identified varicosity was evaluated for colocalization by two independent observers.

A similar design was used for determining colocalization between VGLUT1 and VGLUT2 with either IB4 or CTb. Fibers and varicosities containing the anterograde tracer were examined by confocal microscopy. In each animal, 50 varicosities of each tracer were evaluated in medial NTS in a single section to avoid duplicate counting of fibers extending through multiple tissue sections (n = 3 animals per tracer; total of 150 varicosities each for VGLUT1 and VGLUT2 analyses). Localization of VGLUT immunoreactivity in each identified fiber and varicosity was determined by consensus between two independent observers.

## RESULTS

### CTb and IB4-ir afferents in NTS

Both CTb and IB4 were effective transganglionic anterograde tracers of vagal afferents to the ipsilateral NTS (Fig. 1). CTb injections into the vagus nerve resulted in anterograde labeling within NTS ipsilateral to the injection (Fig. 1A,B). Anterograde labeling was visible as fibers and punctate structures throughout NTS and weakly within the solitary tract (Fig. 1B). After vagal injections of CTb, retrograde labeling was seen in neurons within the dorsal motor nucleus of the vagus

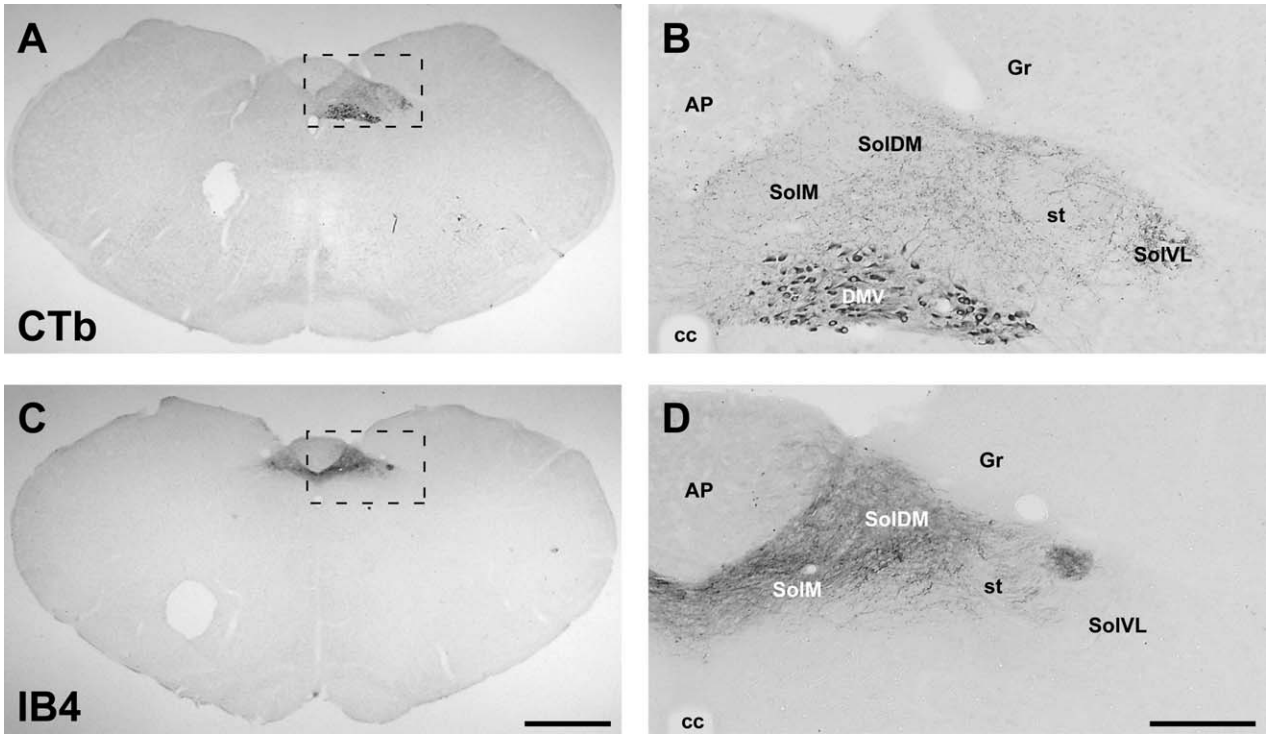


Figure 1. CTb and IB4 label distinct populations of vagal afferents and motor neurons. CTb produced both anterograde and retrograde labeling ipsilateral to the injection (**A,B**). Anterograde labeling with CTb was visible as fibers and puncta within the solitary tract (st) and throughout NTS (B). Retrograde labeling was seen in the somata of neurons in the dorsal motor nucleus of the vagus (DMV; B). In contrast, IB4 injections resulted in only anterograde labeling of small-diameter fibers and puncta (**C,D**), most notably within the medial (SolM) and dorsomedial subnulcei (SolDM) of the ipsilateral NTS (D). AP, area postrema; cc, central canal; SolVL, ventrolateral subnucleus of NTS; Gr, gracile nucleus. Scale bars = 1 mm in C (applies to A,C); 250 μm; in D (applies to B,D).

(Fig. 1B) and in the nucleus ambiguous, particularly the rostral pole (not shown). IB4 injections into the vagus nerve resulted in ipsilateral anterograde labeling of small diameter fibers, most notably within the medial and dorsomedial subnulcei of NTS, with some punctate labeling as well (Fig. 1C,D). Retrograde labeling was not seen following IB4 injections (Fig. 1D).

Although these two anterograde tracers showed distinct labeling patterns in NTS (Fig. 1), there was some overlap in the distribution of fibers within medial NTS. To determine whether these two transganglionic tracers were labeling distinct or overlapping populations of vagal afferents, varicosities and fibers within medial NTS were evaluated following dual injections of both IB4 and CTb into the left cervical vagus (Fig. 2). The tracers labeled distinct populations of fibers. CTB-containing fibers form large varicosities (Fig. 2B), whereas IB4-containing fibers were more abundant and had less prominent varicosities (Fig. 2C). Fibers did not show colocalization of the two anterograde tracers (Fig. 2D). Quantitative analyses confirmed the lack of colocalization of these tracers. We examined segments of nonvaricose lengths of fibers (IB4, length 1,473 μm; CTb, length 964 μm) and found no colocalization. Separate analyses of varicosities showed minimal colocalization; 3% (2/60) of IB4 varicosities contained CTb, and 1% (1/150) of CTb varicosities contained IB4, suggesting that these two tracers identify distinct populations of vagal visceral afferents to NTS.

## Ultrastructural localization of CTb and IB4

The confocal analyses indicate that CTb and IB4 label distinct populations of vagal afferents, so we conducted ultrastructural analyses to verify the types of fibers labeled with each tracer (Fig. 3). Injections of IB4 into the cervical vagus produced labeling in unmeylinated axons (Fig. 3A) as well as axon terminals forming asymmetric synapses (Fig. 3B). IB4 labeling was associated with the plasma membrane and was detected in only some segments of the membrane at the axon terminal (Fig. 3B). CTb labeling was found in myelinated axons (Fig. 3E), unmyelinated axons (Fig. 3C,E), and axon terminals forming asymmetric synapses (Fig. 3D). Within axons, CTb labeling was found within the cytoplasm (Fig. 3C,E), in contrast to IB4 labeling which was

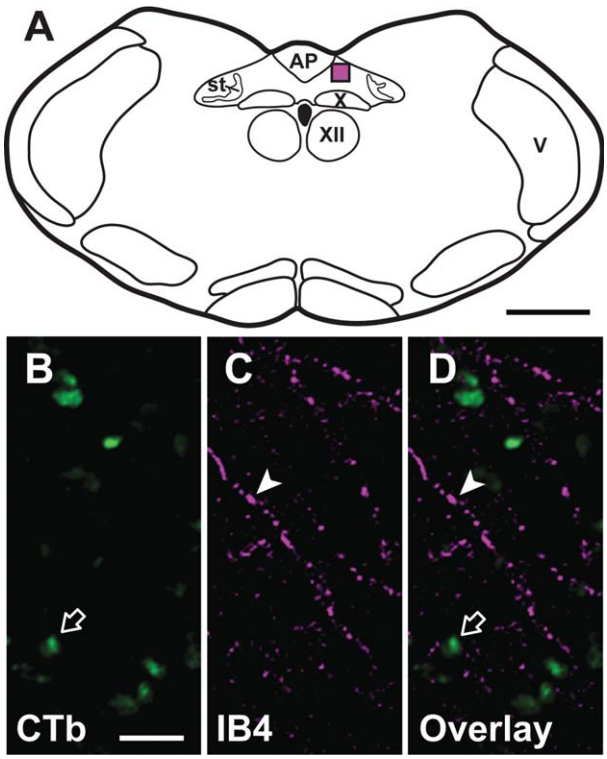


Figure 2. CTb and IB4 label distinct populations of vagal afferents. **A:** Schematic illustration showing region of medial NTS included in analysis at level of area postrema (AP). Confocal micrographs of a single optical section (0.9 μm Z thickness) illustrating anterograde labeling within NTS following microinjections of CTb (**B**; green) and IB4 (**C**; magenta) into the cervical vagus. CTb labeling was seen in large varicosities (open arrows) and occasionally within axonal fibers. IB4 labeling was more abundant and was seen predominantly in fibers (arrowheads) and smaller varicosities. In the overlay (**D**), it is apparent that the two tracers are not colocalized. st, Solitary tract; V, spinal trigeminal nucleus; X, dorsal motor nucleus of the vagus; XII, hypoglossal nucleus. Scale bars = 1 mm in A; 5 μm in B (applies to B–D).

confined to the plasma membrane (Fig. 3A). As seen with IB4, CTb-labeled axon terminals often formed asymmetric synapses and displayed membranous labeling that was largely excluded from the synaptic contact (Fig. 3D). Finally, CTb was found in dorsal motor nucleus of the vagus perikarya (Fig. 3F), where the tracer was largely confined to lysosomes and multivesicular bodies (Fig. 3F).

### VGLUTs in NTS

We examined the distribution of VGLUT1- and VGLUT2-immunoreactive (-ir) profiles within regions of NTS that receive vagal afferents as described above (Fig. 4). In line with prior research (Lin et al., 2004; Corbett et al., 2005; Lachamp et al., 2006), VGLUT1 immunoreactivity was punctate and sparse throughout NTS, with the most abundant immunoreactivity seen within the interstitial and lateral subnuclei as well as within the gracilis nucleus adjacent to NTS (Fig. 4A,B). In contrast, VGLUT2-ir fibers and punctate profiles were detected throughout most subnuclei of NTS, with weaker immunoreactivity seen within the solitary tract (Fig. 4C,D).

### Colocalization of VGLUTs in CTb- and IB4-labeled afferents

To determine which vesicular glutamate transporters were localized to the distinct populations of CTb- and IB4-labeled vagal afferents, we combined immunohistochemistry for either VGLUT1 or VGLUT2 with injections of either CTb or IB4 into the vagus (Figs. 5, 6). Both transporters were found in CTb-labeled vagal afferents (Fig. 5), VGLUT2 being much more abundant (Fig. 5D,E). VGLUT1-ir was found in only a small portion of CTb varicosities (Figs. 5A–C, 7), but VGLUT2-ir was found in most CTb-labeled vagal afferents (Figs. 5D,E, 7). In contrast, neither of the vesicular glutamate transporters was very abundant in IB4-labeled afferents. Very rarely, IB4 fibers contained VGLUT1-ir (Figs. 6A–C, 7), and more IB4-labeled vagal afferents contained VGLUT2-ir (Figs. 6D,E, 7). In summary, the majority of CTb-labeled vagal afferents contained VGLUTs, but most IB4-labeled afferents did not contain detectable levels of either VGLUT (Fig. 7). These findings demonstrate differential localization of VGLUT in anatomically distinct populations of vagal afferents and also suggest that other molecular mechanisms might regulate glutamate release from IB4-containing afferents.

## DISCUSSION

The present studies show that CTb and IB4 can be used as transganglionic anterograde tracers to label distinct populations of vagal afferents, and injections can even be combined in the same animal. Furthermore, the present studies show that CTb and IB4 vagal afferents have distinct vesicular glutamate transporters, suggesting that these two populations may contain distinct molecular mechanisms regulating glutamate release.

In somatic nerves, cholera toxin B subunit (CTb) and isolectin B4 (IB4) label myelinated and unmyelinated fibers, respectively (Todd et al., 2003), although this may not be the case for visceral afferents (Wang et al., 1998). IB4 has also been purported to label only nonpeptide containing c-fibers, but this premise has been disputed for the rat (Price and Flores, 2007). The present study shows that both IB4 and CTb label unmyelinated vagal afferents, with CTb also labeling myelinated

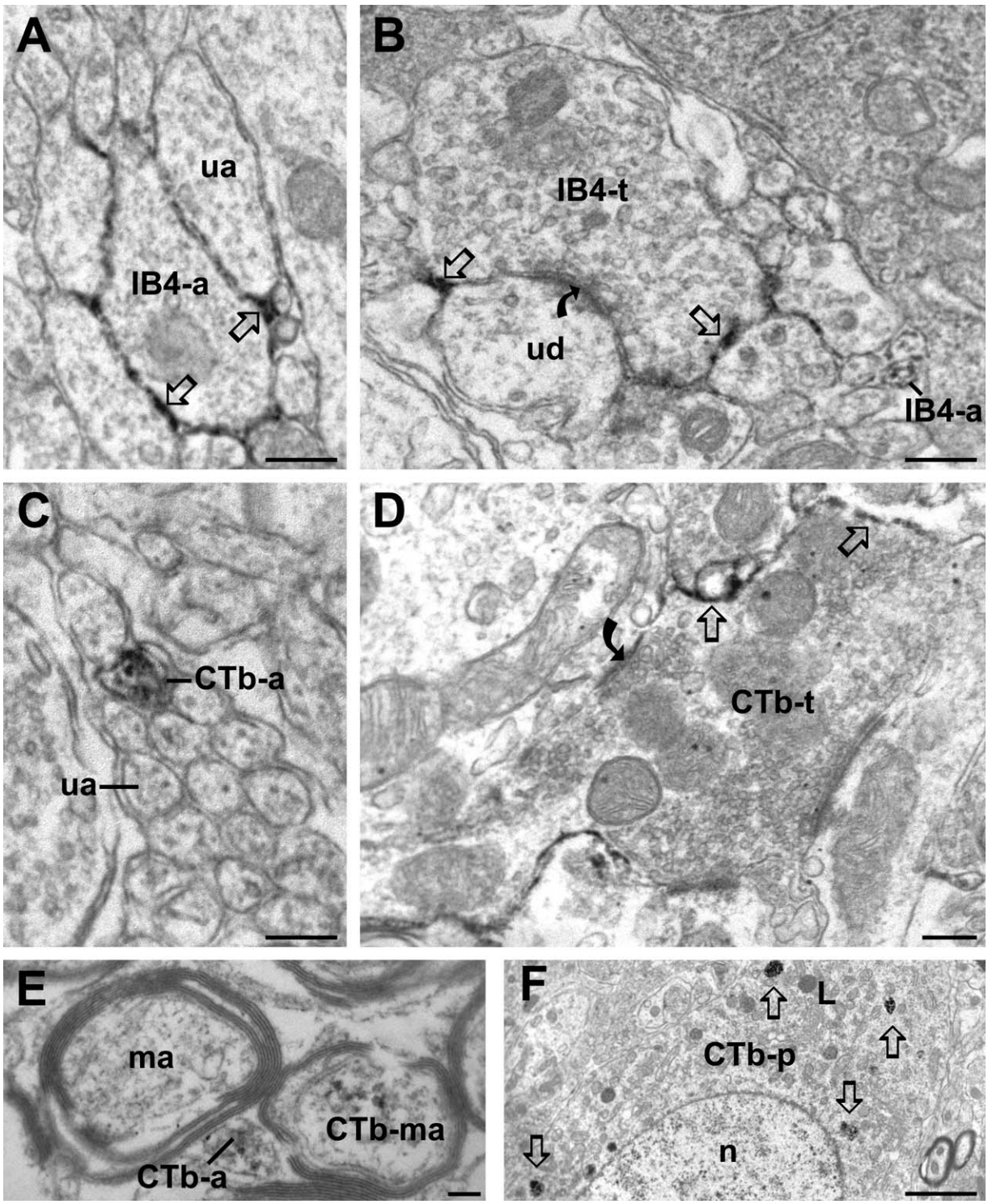


Figure 3. Ultrastructural distributions of IB4 and CTb are distinct. **A,B:** IB4 labeling was seen only in unmyelinated vagal afferents. IB4 labeling was confined to the plasma membrane (straight arrows) of axons (IB4-a) and terminals (IB4-t) but was largely excluded from synapses (curved arrow). ua, unlabeled axon; ud, unlabeled dendrite. **C,D:** CTb labeling was cytoplasmic in axons (CTb-a) and confined to the plasma membrane (straight arrows) of terminals (CTb-t). Labeled terminals often formed asymmetric synapses (curved arrow), consistent with glutamatergic afferents. **E:** In addition to unmyelinated axons (CTb-a), CTb also labeled myelinated axons (CTb-ma). An unlabeled myelinated axon (ma) is seen in close proximity. **F:** Retrograde CTb labeling was also seen in the perikarya of motor neurons (CTb-p). CTb labeling (arrows) was cytoplasmic and was often confined to organelles including lysosomes (L). n, nucleus. Scale bars = 250 nm in A–D; 100 nm in E; 2 μm in F.

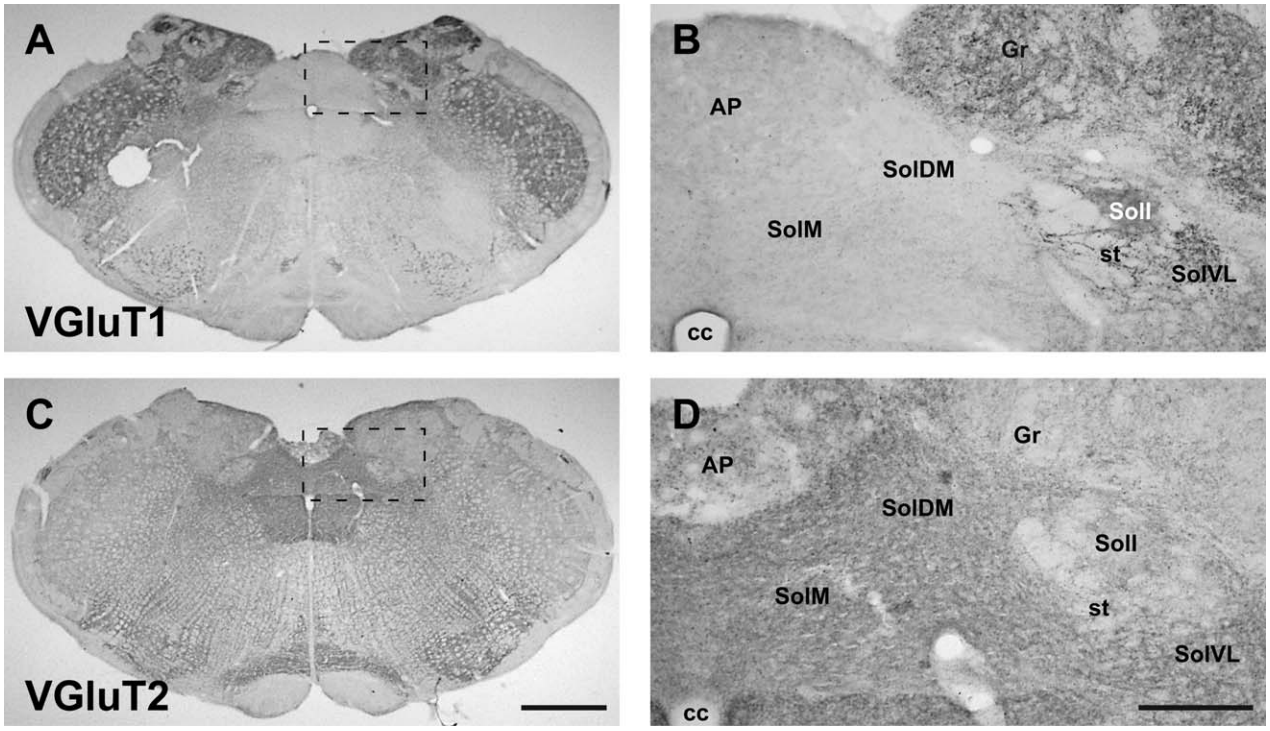


Figure 4. Immunohistochemistry for VGLUT1 and VGLUT2 resulted in complementary labeling patterns throughout NTS. **A,B:** VGLUT1 immunoreactivity was punctate and sparse throughout NTS. In agreement with other studies, the most abundant immunoreactivity was seen within the interstitial (SolI) and the ventrolateral (SolVL) subnuclei of NTS as well as within the gracilis nucleus (Gr). **C,D:** VGLUT2 immunoreactivity was punctate and dense throughout the medial (SolM), dorsomedial (SolDM), and most other subnuclei of NTS, with much weaker labeling seen within the solitary tract (st) and outside NTS. AP, area postrema; cc, central canal. Scale bars = 1 mm in C (applies to A,C); 250 μm; in D (applies to B,D).

afferents. These findings suggest that CTb and IB4 may detect overlapping populations of unmyelinated axons, but in our dual tracing study we rarely found the two tracers colocalized. This could reflect the fact that CTb is found in only a small number of unmyelinated axons. Our results suggest that CTb and IB4 may be useful tools for identifying distinct populations of primarily myelinated and unmyelinated vagal afferents, respectively.

The subcellular distribution of the tracers was also distinct at the ultrastructural level. In axons, CTb was found within the cytoplasm, whereas IB4 appeared to be confined to the plasma membrane. At axon terminals, both CTb and IB4 were found associated with portions of the plasma membrane away from the synaptic junction. This localization makes identification of axon terminals more difficult to assess than anterograde tracers that fill the cytoplasm and axon terminal (Aicher et al., 2000) but also leaves the axon terminals available for ready visualization. Retrograde transport of CTb was largely confined to lysosomes and dense-core vesicles as we have seen previously with ultrastructural analysis of other retrograde tracers (Aicher et al., 1995).

VGLUT1 and -2 are generally found in a complementary distribution throughout the CNS and have been assumed to be present in all axon terminals that use glutamate as a neurotransmitter. Both somatic and visceral primary afferents are thought to use glutamate as a neurotransmitter, so these afferents would be expected to contain a VGLUT. The distribution of VGLUTs in different populations of afferents has been extensively studied, and analyses have examined distributions on the basis of fiber type, afferent function, and colocalization with other neurotransmitters (Lachamp et al., 2006; Lin and Talman, 2006; Brumovsky et al., 2012). VGLUT1 has been reported to be most abundant in mechanosensory/proprioceptive primary spinal afferents (Landry et al., 2004) and absent from nonpeptidergic (IB4) and peptidergic (SP or somatostatin) spinal primary afferents (Todd 2003). However, these latter findings conflict with other studies reporting the presence of VGLUTs in IB4 and peptidergic (CGRP) fibers (Alvarez et al., 2004). Some myelinated afferents (identified with CTb) in deeper spinal dorsal horn laminae (Todd et al., 2003), as well as some trigeminal afferents (Li

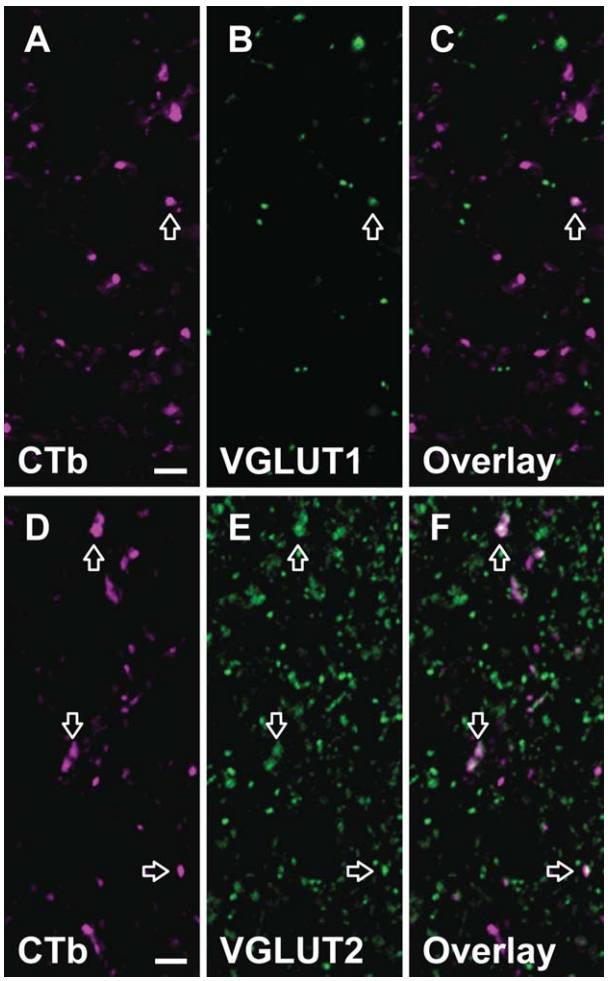


Figure 5. CTb-labeled vagal afferents frequently contain VGLUT2. Localization of VGLUT1 and VGLUT2 in vagal afferents detected with CTb. **A–C:** CTb afferents (magenta) rarely (9%, 13/150) contained VGLUT1-ir (green) as shown in the overlay (C) as white (arrows). **D–F:** In contrast, many (83%, 124/150) CTb afferents (D, magenta) contained VGLUT2-ir (E, green), which are seen as white (arrows) in the overlay (F). Each series of confocal micrographs is a Z-projection of three consecutive overlapping optical sections for a total Z thickness of 1.8 μm. Assessments of colocalization were conducted on single optical sections, and Z stacks were used only for illustration purposes, because single optical sections rarely reveal continuous fibers. Scale bars = 5 μm in A (applies to A–C); 5 μm; in D (applies to D–F).

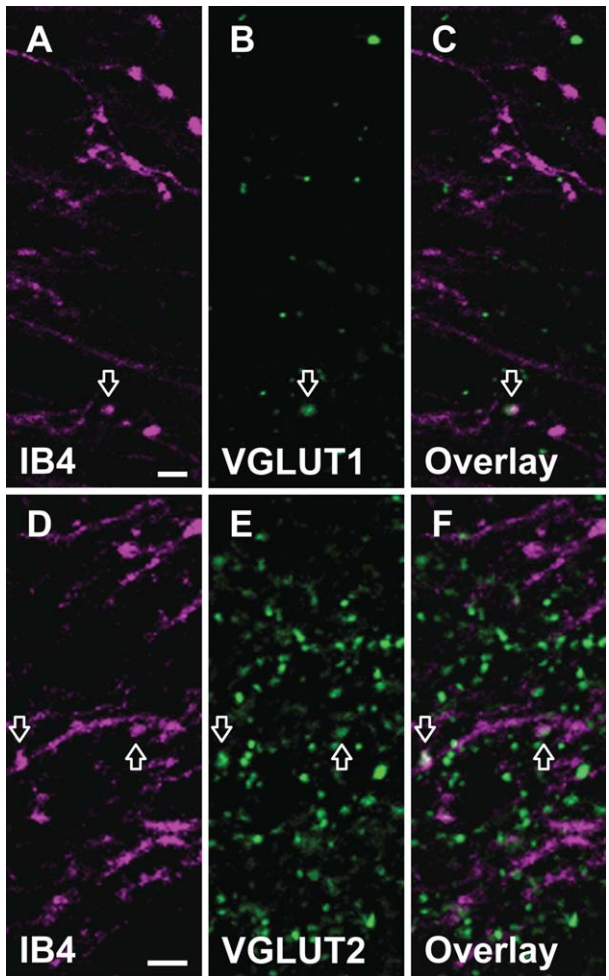


Figure 6. IB4-labeled vagal afferents only occasionally contained VGLUT1 or VGLUT2. IB4 afferents (magenta) are found in regions containing VGLUT1 (green, **A–C**) and VGLUT2 (green, **D–F**). Only 5% (7/150) of IB4 afferents (A, magenta) contained VGLUT1-ir (B, green) as indicated in the overlay (C). IB4 afferents (D, magenta) were more likely (21%, 31/150) to contain VGLUT2-ir (E, green) as indicated (white, arrows) in the overlay (F). Scale bars = 5 μm in A (applies to A–C); 5 μm; in D (applies to D–F).

et al., 2003), have been reported to contain both VGLUT1 and VGLUT2.

Autonomic afferents from most visceral organs terminate in the NTS. Although most glutamatergic synapses in the NTS have been reported to contain VGLUT2, VGLUT1 terminals have also been reported (Lachamp et al., 2006). Corbett and colleagues (2005) demonstrated that cardiac afferent neurons (both myelinated and unmyelinated) labeled with CTb injected into the pericardial sac contained predominantly VGLUT1-ir, and only rarely contain VGLUT2-ir or VGLUT3-ir. In contrast, most other vagal afferents, identified with CTb injections into the aortic nerve, stomach, or nodose ganglion, more frequently contained VGLUT2-ir than VGLUT1-ir (Corbett et al., 2005). A recent study of bladder sensory afferents whose cell bodies are located in the dorsal root ganglia (Brumovsky et al., 2012) showed that these visceral afferents also contained primarily VGLUT2. These results are consistent with our results showing that CTb-labeled visceral vagal afferents contain primarily VGLUT2. However, our findings with IB4 suggest that another population of vagal afferents that are unmyelinated and are not detected with CTb might have VGLUT1, as well as other mechanisms for releasing glutamate.

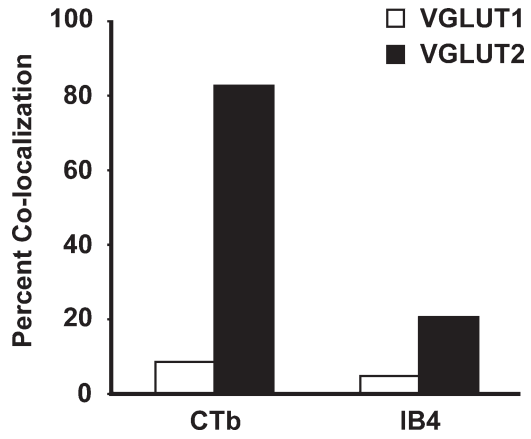


Figure 7. Summary graph illustrating the percentage of anterogradely labeled vagal afferent varicosities that also contained either VGLUT1 or VLGUT2 immunoreactivity. VGLUT1 immunoreactivity was colocalized with 9% of CTb-ir varicosities (13/150) and only 5% of IB4 varicosities. VGLUT2 immunoreactivity was colocalized with 83% of CTb-ir varicosities (124/150) and only 21% of IB4 varicosities (31/150).

Recent studies have demonstrated that glutamate release may be regulated by a variety of molecular mechanisms and even within the same axon terminals, different populations of vesicles may be released under different conditions (Chung and Kavalali, 2006). To date, the function underlying the segregation, or colocalization, of different vesicular glutamate transporters in different types of afferents is unclear. It has been speculated that isoforms of VGLUT may produce varying rates of vesicle refilling and thus lead to different levels of synaptic plasticity (Takamori, 2006). Vesicular glutamate transporters have also been implicated in vesicular synergy (El Mestikawi et al., 2011), leading to modulation of neurotransmission for other molecules that are colocalized with glutamate.

In light of recent insights into the complex regulation of glutamate release and its potential modulation by other molecules, such as TRPV1 (Peters et al., 2010), the current findings suggest that distinct populations of vagal afferents may possess multiple molecular mechanisms for the regulation of neurotransmitter release and that these molecules may undergo complex interactions, which might also be altered under pathological conditions (Brumovsky et al., 2007; Llewellyn-Smith et al., 2007). The work of Andresen and colleagues (2012) opens the intriguing possibility that glutamate release from primary visceral vagal afferents is directly modulated by temperature-induced opening of TRPV1 channels, which act as cation channels and can independently cause glutamate release. There is conflicting evidence in the literature with regard to whether distinct neurotransmitter transporters are localized to individual synaptic vesicles or whether distinct populations of vesicles exist within the same axon terminal (El Mestikawi et al., 2011). Further studies are needed to determine the subcellular localization of various molecules that may modulate the release of glutamate from vagal afferents in the NTS. Our studies suggest that distinct molecular mechanisms may exist for myelinated and unmyelinated afferents.

## ACKNOWLEDGMENTS

The authors thank Dr. Michael C. Andresen for comments on the manuscript.

## CONFLICT OF INTEREST STATEMENT

The authors have no conflicts of interest to declare.

## ROLE OF AUTHORS

All authors had full access to all the data in the study and take responsibility for the integrity of the data and the accuracy of the data analysis. Study concept and design: SAA. Acquisition of data: JFC, SMH. Analysis and interpretation of data: SMH, SAA. Drafting of the manuscript: SAA. Critical revision of the manuscript: SMH, JFC. Obtained funding: SAA. Study supervision: SAA.

## LITERATURE CITED

Aicher SA, Reis DJ, Nicolae R, Milner TA. 1995. Monosynaptic projections from the medullary gigantocellular reticular formation to sympathetic preganglionic neurons in the thoracic spinal cord. J Comp Neurol 363:563–580.

Aicher SA, Sharma S, Cheng PY, Pickel VM. 1997. The N-methyl-D-aspartate (NMDA) receptor is postsynaptic to substance P-containing axon terminals in the rat superficial dorsal horn. Brain Res 772:71–81.

Aicher SA, Sharma S, Pickel VM. 1999. N-methyl-D-aspartate receptors are present in vagal afferents and their dendritic targets in the nucleus tractus solitarius. Neuroscience 91:119–132.

Aicher SA, Goldberg A, Sharma S, Pickel VM. 2000. $\mu$-Opioid receptors are present in vagal afferents and their dendritic targets in the medial nucleus tractus solitarius. J Comp Neurol 422:181–190.

Alvarez FJ, Villalba RM, Zerda R, Schneider SP. 2004. Vesicular glutamate transporters in the spinal cord, with special reference to sensory primary afferent synapses. J Comp Neurol 472:257–280.

Ambalavanar R, Morris R. 1993. An ultrastructural study of the binding of an alpha-D-galactose specific lectin from *Griffonia simplicifolia* to trigeminal ganglion neurons and the trigeminal nucleus caudalis in the rat. Neuroscience 52:699–709.

Andresen MC, Kunze DL. 1994. Nucleus tractus solitarius—gateway to neural circulatory control. Annu Rev Physiol 56:93–116.

Andresen MC, Hofmann ME, Fawley JA. 2012. Invited review: the un-silent majority—TRPV1 drives "spontaneous" transmission of unmyelinated primary afferents within

cardiorespiratory NTS. Am J Physiol Regul Integr Comp Physiol 303:R1207–R1216.

Bailey TW, Hermes SM, Andresen MC, Aicher SA. 2006. Cranial visceral afferent pathways through the nucleus of the solitary tract to caudal ventrolateral medulla or paraventricular hypothalamus: target-specific synaptic reliability and convergence patterns. J Neurosci 26:11893–11902.

Bellocchio EE, Reimer RJ, Fremeau RT Jr, Edwards RH. 2000. Uptake of glutamate into synaptic vesicles by an inorganic phosphate transporter. Science 289:957–960.

Brumovsky P, Watanabe M, Hokfelt T. 2007. Expression of the vesicular glutamate transporters-1 and -2 in adult mouse dorsal root ganglia and spinal cord and their regulation by nerve injury. Neuroscience 147:469–490.

Brumovsky PR, Seal RP, Lundgren KH, Seroogy KB, Watanabe M, Gebhart GF. 2012. Expression of vesicular glutamate transporters in sensory and autonomic neurons innervating the mouse urinary bladder. J Urol 189:2342–2349.

Caterina MJ, Julius D. 1999. Sense and specificity: a molecular identity for nociceptors. Curr Opin Neurobiol 9:525–530.

Chomsung RD, Petry HM, Bickford ME. 2008. Ultrastructural examination of diffuse and specific tectopulvinar projections in the tree shrew. J Comp Neurol 510:24–46.

Chung C, Kavalali ET. 2006. Seeking a function for spontaneous neurotransmission. Nat Neurosci 9:989–990.

Corbett EK, Sinfield JK, McWilliam PN, Deuchars J, Batten TF. 2005. Differential expression of vesicular glutamate transporters by vagal afferent terminals in rat nucleus of the solitary tract: projections from the heart preferentially express vesicular glutamate transporter 1. Neuroscience 135:133–145.

El Mestikawi S, Wallen-Mackenzie A, Fortin GM, Descarries L, Trudeau LE. 2011. From glutamate corelease to vesicular synergy: vesicular glutamate transporters. Nat Rev Neurosci 12:204–216.

Fishman PH. 1982. Role of membrane gangliosides in the binding and action of bacterial toxins. J Membrane Biol 69:85–97.

Fremeau RT Jr, Voglmaier S, Seal RP, Edwards RH. 2004. VGLUTs define subsets of excitatory neurons and suggest novel roles for glutamate. Trends Neurosci 27:98–103.

Gras C, Herzog E, Bellenchi GC, Bernard V, Ravassard P, Pohl M, Gasnier B, Giros B, El Mestikawy S. 2002. A third vesicular glutamate transporter expressed by cholinergic and serotoninergic neurons. J Neurosci 22:5442–5451.

Hegarty DM, Tonsfeldt K, Hermes SM, Helfand H, Aicher SA. 2010. Differential localization of vesicular glutamate transporters and peptides in corneal afferents to trigeminal nucleus caudalis. J Comp Neurol 518:3557–3569.

Kalia M, Mesulam M-M. 1980. Brain stem projections of sensory and motor components of the vagus complex in the cat: I. The cervical vagus and nodose ganglion. J Comp Neurol 193:435–465.

Kalia M, Sullivan JM. 1982. Brainstem projections of sensory and motor components of the vagus nerve in the rat. J Comp Neurol 211:248–264.

Kitchener PD, Wilson P, Snow PJ. 1993. Selective labelling of primary sensory afferent terminals in lamina II of the dorsal horn by injection of *Bandeiraea simplicifolia* isolectin $B_4$ into peripheral nerves. Neuroscience 54:545–551.

Lachamp P, Crest M, Kessler JP. 2006. Vesicular glutamate transporters type 1 and 2 expression in axon terminals of the rat nucleus of the solitary tract. Neuroscience 137:73–81.

Landry M, Bouali-Benazzouz R, El MS, Ravassard P, Nagy F. 2004. Expression of vesicular glutamate transporters in rat lumbar spinal cord, with a note on dorsal root ganglia. J Comp Neurol 468:380–394.

Lefler Y, Arzi A, Reiner K, Sukhotinsky I, Devor M. 2008. Bulbospinal neurons of the rat rostromedial medulla are highly collateralized. J Comp Neurol 506:960–978.

Li JL, Xiong KH, Dong YL, Fujiyama F, Kaneko T, Mizuno N. 2003. Vesicular glutamate transporters, VGluT1 and VGluT2, in the trigeminal ganglion neurons of the rat, with special reference to coexpression. J Comp Neurol 463:212–220.

Lin LH, Talman WT. 2006. Vesicular glutamate transporters and neuronal nitric oxide synthase colocalize in aortic depressor afferent neurons. J Chem Neuroanat 32:54–64.

Lin LH, Edwards RH, Fremeau RT, Fujiyama F, Kaneko T, Talman WT. 2004. Localization of vesicular glutamate transporters and neuronal nitric oxide synthase in rat nucleus tractus solitarii. Neuroscience 123:247–255.

Llewellyn-Smith IJ, Pilowsky P, Minson JB, Chalmers J. 1995. Synapses on axons of sympathetic preganglionic neurons in rat and rabbit thoracic spinal cord. J Comp Neurol 354:193–208.

Llewellyn-Smith IJ, Martin CL, Fenwick NM, DiCarlo SE, Lujan HL, Schreihofer AM. 2007. VGLUT1 and VGLUT2 innervation in autonomic regions of intact and transected rat spinal cord. J Comp Neurol 503:741–767.

Mei N, Condamin M, Boyer A. 1980. The composition of the vagus nerve of the cat. Cell Tissue Res 209:423–431.

Melone M, Burette A, Weinberg RJ. 2005. Light microscopic identification and immunocytochemical characterization of glutamatergic synapses in brain sections. J Comp Neurol 492:495–509.

Okada E, Maeda T, Watanabe T. 1982. Immunocytochemical study on cholera toxin binding sites by monoclonal anti-cholera toxin antibody in neuronal tissue culture. Brain Res 242:233–241.

Peters A, Palay SL, Webster HD. 1991. The fine structure of the nervous system: neurons and their supporting cells, 3rd ed. New York: Oxford.

Peters JH, McDougall SJ, Fawley JA, Smith SM, Andresen MC. 2010. Primary afferent activation of thermosensitive TRPV1 triggers asynchronous glutamate release at central neurons. Neuron 65:657–669.

Pickel VM. 1981. Immunocytochemical methods. In: Heimer L, Robards MJ, editors. Neuroanatomical tract tracing methods. New York: Plenum. p 483–509.

Price TJ, Flores CM. 2007. Critical evaluation of the colocalization between calcitonin gene-related peptide, substance P, transient receptor potential vanilloid subfamily type 1 immunoreactivities, and isolectin B4 binding in primary afferent neurons of the rat and mouse. J Pain 8:263–272.

Ramer MS. 2008a. Anatomical and functional characterization of neuropil in the gracile fasciculus. J Comp Neurol 510: 283–296.

Ramer MS. 2008b. Anatomical and functional characterization of neuropil in the gracile fasciculus. J Comp Neurol 510: 283–296.

Renick SE, Kleven DT, Chan J, Stenius K, Milner TA, Pickel VM, Fremeau RT Jr. 1999. The mammalian brain high-affinity L-proline transporter is enriched preferentially in synaptic vesicles in a subpopulation of excitatory nerve terminals in rat forebrain. J Neurosci 19:21–33.

Schnell SA, Wessendorf MW. 2008. Coexpression of the mu-opioid receptor splice variant MOR1C and the vesicular glutamate transporter 2 (VGLUT2) in rat central nervous system. J Comp Neurol 508:542–564.

Shehab SA. 2009. Acute and chronic sectioning of fifth lumbar spinal nerve has equivalent effects on the primary

afferents of sciatic nerve in rat spinal cord. J Comp Neurol 517:481–492.

Starkey ML, Davies M, Yip PK, Carter LM, Wong DJ, McMahon SB, Bradbury EJ. 2009. Expression of the regeneration-associated protein SPRR1A in primary sensory neurons and spinal cord of the adult mouse following peripheral and central injury. J Comp Neurol 513: 51–68.

Sugimoto T, Fujiyoshi Y, He YF, Xiao C, Ichikawa H. 1997. Trigeminal primary projection to the rat brain stem sensory trigeminal nuclear complex and surrounding structures revealed by anterograde transport of cholera toxin B subunit-conjugated and *Bandeiraea simplicifolia* isolectin B4-conjugated horseradish peroxidase. Neurosci Res 28: 361–371.

Takamori S. 2006. VGLUTs: "exciting" times for glutamatergic research? Neurosci Res 55:343–351.

Talman WT, Perrone MH, Reis DJ. 1980. Evidence for L-glutamate as the neurotransmitter of primary baroreceptor afferent nerve fibers. Science 209:813–815.

Todd AJ, Hughes DI, Polgar E, Nagy GG, Mackie M, Ottersen OP, Maxwell DJ. 2003. The expression of vesicular glutamate transporters VGLUT1 and VGLUT2 in neurochemically defined axonal populations in the rat spinal cord with emphasis on the dorsal horn. Eur J Neurosci 17:13–27.

Varoqui H, Schafer MK, Zhu H, Weihe E, Erickson JD. 2002. Identification of the differentiation-associated $Na^+$/PI transporter as a novel vesicular glutamate transporter expressed in a distinct set of glutamatergic synapses. J Neurosci 22:142–155.

Wang H, Rivero-Melian C, Robertson B, Grant G. 1994. Transganglionic transport and binding of the isolectin B4 from *Griffonia simplicifolia* I in rat primary sensory neurons. Neuroscience 62:539–551.

Wang HF, Shortland P, Park MJ, Grant G. 1998. Retrograde and transganglionic transport of horseradish peroxidase-conjugated cholera toxin B subunit, wheatgerm agglutinin and isolectin B4 from *Griffonia simplicifolia* I in primary afferent neurons innervating the rat urinary bladder. Neuroscience 87:275–288.